

Intra-Variable Handwriting Inspection Reinforced with Idiosyncrasy Analysis

Chandranath Adak, *Member, IEEE*, Bidyut B. Chaudhuri, *Life Fellow, IEEE*, Chin-Teng Lin, *Fellow, IEEE*, and Michael Blumenstein, *Senior Member, IEEE*

Abstract—In this paper, we work on intra-variable handwriting, where the writing samples of an individual can vary significantly. Such within-writer variation throws a challenge for automatic writer inspection, where the state-of-the-art methods do not perform well. To deal with intra-variability, we analyze the idiosyncrasy in individual handwriting. We identify/verify the writer from highly idiosyncratic text-patches. Such patches are detected using a deep recurrent reinforcement learning-based architecture. An idiosyncratic score is assigned to every patch, which is predicted by employing deep regression analysis. For writer identification, we propose a deep neural architecture, which makes the final decision by the idiosyncratic score-induced weighted average of patch-based decisions. For writer verification, we propose two algorithms for patch-fed deep feature aggregation, which assist in authentication using a triplet network. The experiments were performed on two databases, where we obtained encouraging results.

Index Terms—Deep Learning, Idiosyncratic Writing, Intra-variable Handwriting, Reinforcement Learning, Writer Identification, Writer Verification.

I. INTRODUCTION

HANDWRITING is still considered as strong evidence in criminal courts of many countries due to its solid impact on behavioral biometrics [1], [2]. Therefore, for the last four decades, research on handwriting inspection has been of great interest in forensics. Moreover, the computational approaches are embedded in handwriting forensics owing to booming automation since the late 20th century. Besides, the "9/11" and "2001 Anthrax" attacks have reignited the computational handwriting forensics research [3].

From the forensic perspective, the handwritten specimen can be found mostly as an offline sample in the form of a threat letter, suicide note, forged manuscript, etc. [1]. Therefore, in this paper, we focus on offline handwriting. The offline handwriting analysis is more challenging compared to online writing due to absence of stroke trajectory, writing pressure, velocity, etc.

In computational handwriting analysis, the focus during the last decade and the first half of the current decade were on handcrafted features. The deep neural net derived feature-based studies have thrived during the latter half of the current

decade [4]. Although the past researches on writer inspection have produced some encouraging results, the major works have been performed on inter-variable writing [5]. The computational research on intra-variability of handwriting has been somewhat overlooked. However, handwriting intra-variability is observed rather frequently due to some mechanical, physical, and psychological factors of the writers [6]. To the best of our knowledge, only one computational experiment has been performed on intra-variability due to Adak et al. [6]. In that study, the authors experimentally showed that the general handcrafted and deep feature-based models did not work well on intra-variable writer inspection, i.e., training/testing on disparate writing styles. At this point, our paper comes into place to identify/verify the writer from intra-variable writing. Some important circumstances where our method is relevant are as follows.

(i) *Absent data*: In forensics and biometrics [1], [7], for a writer examination system, a specific writing style/type of an individual may be absent during training. Now, the system may be required for testing on that particular type of writing.

(ii) *Discovered manuscript*: In archival science and library science, the authorship is checked when an unpublished historical cultural manuscript is discovered. The manuscript may contain some unknown writing styles of a claimant [7]. A system may be essential to verify such a claimant.

(iii) *Healthcare*: Some diseases, e.g., Parkinson's, Dyslexia, Alzheimer's, Dysgraphia, Tourette syndrome, etc., affect the handwriting of an individual [8], [9]. Therefore, the writing of a patient changes over multiple stages of disease progression. A system that can understand such intra-variability, may be needed to analyze such disease development. Our proposed system has the potential to address such real-world issues.

In Fig. 1, we present some examples on intra-variable and inter-variable handwriting. The samples of the upper row (Fig.

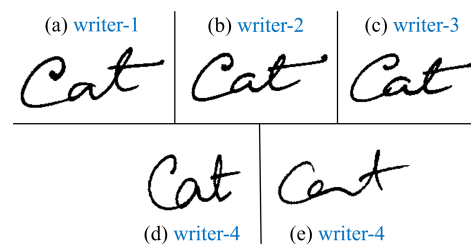


Fig. 1: (a), (b), (c): 3 samples written by 3 different writers: *low inter-variability*; (d), (e): 2 samples written by the same writer: *high intra-variability*.

C. Adak is with the Centre for Data Science, JIS Institute of Advanced Studies and Research, JIS University, India-700091, and also with School of Computer Science, FEIT, University of Technology Sydney, Australia-2007. (e-mail: chandra@jisiasr.org).

B. B. Chaudhuri is with Dept. of CSE, Techno India University, India-700091, and also with CVPR Unit, Indian Statistical Institute, India-700108.

C.-T. Lin and M. Blumenstein are with the Centre for AI, School of Computer Science, FEIT, University of Technology Sydney, Australia-2007.

This paper is a preprint version of DOI: 10.1109/TIFS.2020.2991833

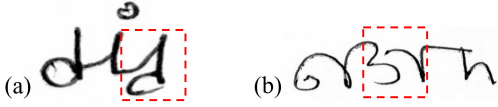


Fig. 2: Idiosyncratic writing samples in (a) *English* and (b) *Bengali* scripts, marked in red dashed boxes: (a) eccentric cursive stroke to scribble character ‘d’, (b) queer penning of the Bengali character containing intermittent stroke.

1:(a)-(c) appear to be structurally similar; however, these are written by three different writers. It depicts the *low inter-variability* which is mostly performed with the intention of writing/signature-forgery [10]. Here, writer-2 (Fig. 1:(b)) and writer-3 (Fig. 1:(c)) try to forge the inscription of writer-1 (Fig. 1:(a)). In Fig. 1:(d), (e), two writing samples appear to be dissimilar, but both are written by the same writer, i.e., writer-4. It portrays *high intra-variability*. In this paper, we are concerned with such high intra-variability in contrast with the past works [3], [5].

For intra-variable handwriting inspection, the idiosyncrasy analysis [11] of handwriting may be useful, since the forensic experts and paleographers follow quite a similar manual approach [1]. Idiosyncrasy analysis of handwriting refers to examining the eccentricity in individual writing style. The originating Greek word of idiosyncrasy is "*idiosunkrasia*", i.e. *idios* (own, private) + *sun* (with) + *krasis* (mixture), which denotes the "distinctive or peculiar feature or characteristic"¹ of an individual. We observe that almost every writer scribbles some character-texts in a peculiar style, which may be useful to inspect the writer on intra-variable writing. In Fig. 2:(a) and (b), we present two examples in English and Bengali scripts, where the writing idiosyncrasy is marked by red dashed boxes. Usually, to write the English character ‘d’, at first the lower loop is scribbled, then the vertical straight line is drawn. However, in Fig. 2:(a), to write ‘d’, the vertical line is penned before the loop creation. Therefore, here, instead of the lower part (loop), the upper part (vertical line) of the ‘d’ creates a continuity with the previous character, which represents the individual idiosyncrasy. In Fig. 2:(b), to write the Bengali character ‘ঈ’, an unnecessary ink-stroke gap makes the character penning highly idiosyncratic (IdS).

In [11], a preliminary work on idiosyncrasy analysis is performed, which did not deal with intra-variable writing; however, it has provided an insight that such analysis has a positive impact on Writer Identification (WI). The authors modeled the idiosyncrasy analysis task into a classification problem to classify the text-patches into multiple classes defined by an IdS score. Their patch selection is mostly based on a sequential search with character-level information. In the current paper, we formulate the idiosyncrasy analysis task in a more sophisticated way, where we predict the score through deep regression [12], and select highly IdS patches using Reinforcement Learning (RL) [13].

In this paper, we inspect the writer from the IdS patches, instead of using all the patches that was performed in [6]. For writer inspection, a handwritten document is examined. In this paper, the examination involves the identification and

verification of a writer. In the WI task, we find the correct writer-id of a questioned handwritten sample from multiple samples of different writers of a database. As a matter of fact, WI is a multi-class classification problem, where we need to find an unknown writer class among multiple writer classes. In the Writer Verification (WV) task, we authenticate an asked handwriting sample whether it has been written by a particular writer or not. Therefore, WV is a binary classification problem. For WI and WV, we use some deep learning-based features. We perform the experiment on the database used in [6], which contains relatively high intra-variable Bengali offline handwriting. The outcome of our method is better than that presented in [6] (refer to Section VI).

The contributions of our current research are briefly mentioned as follows:

(i) The state-of-the-art methods including [6] do not perform so well to inspect the writer on highly intra-variable handwriting. The method proposed in this paper performs better than the past techniques. Merging the idiosyncrasy analysis with intra-variable handwriting inspection is newly proposed here.

(ii) We find highly IdS patches, and perform writer inspection on these patches only. To obtain an IdS score of a patch, we use a deep-feature induced regression analysis [12]. For highly IdS patch localization, we employ RL [13]. In RL, we propose a novel internal reward shaping function which is computed using the IdS score (refer to Section III).

(iii) For WI, combining the decisions obtained from individual patches is a new contribution, where the overall decision is made by the IdS score-fed weighted average of the individual patch-based decisions (refer to Section IV).

(iv) For WV, we propose two separate methods (MAF and XAF) for generating a combined page-level deep feature from multiple patch-level features (refer to Section V).

The rest of the paper is organized as follows. Section II explores the related work in the area. Section III discusses our proposed method for idiosyncrasy analysis. Then Sections IV and V describe our WI and WV methods. The following Section VI deals with the experiments and results of our proposed method. Finally, Section VII concludes this paper.

II. RELATED WORK

To the best of our knowledge and online/offline searching capacity, there is no direct computational work on intra-variable handwriting inspection for WI/WV except [6], in the literature. The notable state-of-the-art methods [5], [14] did not tackle the writer-inspection problem concerning within-writer variation, which is the main focus of this paper. Only Adak et al. [6] reported this issue after performing an empirical study, where they showed that major handcrafted feature, and deep feature-based writer inspection models, did not perform well on intra-variable handwriting. The challenge here is the training and testing executed on disparate writing styles of an individual.

However, in this section, we briefly mention some significant state-of-the-art writer inspection methods. A comprehensive survey on writer inspection up to the year 1989 is reported in [14]. The overview of the recent offline writer investigations

¹<https://en.oxforddictionaries.com> , last retrieved on 30 March 2020.

can be found in [5]. The writer-inspection techniques can broadly be divided into two categories: (i) handcrafted feature-based models [3], [15]–[22] and (ii) deep feature-based models [6], [23]–[26].

(i) *Handcrafted feature-based models*: Among handcrafted feature-based methods, the macro-micro feature-based model of Srihari et al. [15] was well appreciated due to successful writer inspection on a U.S. population of 1500 from various demographics. Their macro features were mostly based on some statistical stroke information about entropy, slope, contour, text-line height, slant, etc. The micro features contained the chain code regarding gradient, structural and concavity-based stroke characteristics. Bulacu and Schomaker [3] proposed some handcrafted textural and allographic features. Their contour-hinge textural feature is very popular in the community due to its good performance. Besides, the grapheme emission PDF (Probability Distribution Function) allographic feature works well for writer inspection.

He and Schomaker [16] extracted curvature-free handcrafted features based on LBP (Local Binary Patterns)-runs over the image and line distribution (COLD: Cloud of Line Distribution) over dominant points of the contour. Wu et al. [17] detected SIFT (Scale-Invariant Feature Transform) keypoints, and obtained their SDS (SIFT Descriptor Signature) and SOH (Scale and Orientation Histogram) to inspect the writer. Some other handcrafted features, e.g., LBP and its variants [18], [19], LPQ (Local Phase Quantization) [18], oBIF (oriented Basic Image Features) [20], K-Adjacent Segments [21], Zernike moments encoded into VLAD (Vectors of Locally Aggregated Descriptors) [22], etc. have been used in the literature.

(ii) *Deep feature-based models*: The deep features are mostly extracted by a CNN (Convolutional Neural Network). Christlein et al. [23] produced the CNN-based local activation features and a GMM (Gaussian Mixture Model)-based super-vector for writer inspection. Tang and Wu [24] extracted deep features using CNN and accomplished the writer-inspection task by employing a joint Bayesian technique. He et al. [25] obtained CNN-based features from a handwritten word image. Their main writer inspection task took the transfer learning benefit from another auxiliary task (e.g., WR: Word Recognition, WLE: Word Length Estimation, etc.), where adaptive convolutional layers were used during the transfer. Fiel and Sablatnig [26] used a CaffeNet for deep feature extraction and the nearest neighbor classifier for writer inspection. In [6], an empirical study was conducted where some major deep architectures, such as SqueezeNet, GoogLeNet, Xception Net, VGG-16, ResNet-101, etc. were analyzed for deep feature extraction.

III. IDIOSYNCRASY ANALYSIS

In this section, we perform idiosyncrasy analysis, where the objective is to find some highly idiosyncratic patches from a handwritten text sample, which can assist in writer inspection.

A. Idiosyncratic Opinion Score

Before finding the highly idiosyncratic (IdS) patches, we need to define an idiosyncrasy measure, based on which we

can mark the respective patches as high or low. We adopt the idea of [11] to define this measure, i.e., subjective opinion score [27]. Now, we discuss the procedure to obtain the ground-truth score.

For ground-truthing, on a given text-patch (p_t), several handwriting experts provided their opinion scores ($I_j^{(t)}$) within a continuous range of $[I_L, I_H]$; $I_L, I_H \in \mathbb{R}^+$. Here, we choose $I_L = 0$, $I_H = 10$. The arithmetic mean ($I_\mu^{(t)}$) of these scores is the *idiosyncratic opinion score* of a patch p_t , i.e., $I_\mu^{(t)} = \frac{1}{e} \sum_{j=1}^e I_j^{(t)}$; where $e > 1$ is the total number of experts who put score on a patch p_t . For our task, $e \geq 30$, i.e., at least 30 experts put individual scores on a patch. Adak et al. [11] partitioned the score range $[I_L, I_H]$ into n_I number of bins (classes) of equal width and modeled a classification task to find highly IdS patch classes. We work here differently by using regression analysis, where we predict the IdS score of a patch. In this paper, the score interval $[I_L, I_H]$ is normalized into $[0, 1]$ to produce normalized IdS score i_t of patch p_t , i.e., $i_t = \frac{I_\mu^{(t)} - I_L}{I_H - I_L}$; $0 \leq i_t \leq 1$. A patch p_t with $i_t = 1$ refers to the highest IdS patch, whereas $i_t = 0$ refers to the lowest one. As a matter of fact, on a page, multiple patches with the same IdS score may present. The score i_t assists in automated detection of highly IdS patches, as well as in writer inspection, as described in the following subsections.

B. Detecting Idiosyncratic Patches

A handwritten page is scanned to be used as an input image. Now, the task is to detect the IdS patches from the input image. We consider the problem as a decision making process where an agent interacts with a visual environment, viz., scanned handwritten page, to detect the target patches. At each timestep, the agent partially observes the input image and decides where to focus on the next timestep.

We cast this problem as a partially observable MDP (Markov Decision Process) since it allows the agent to make a decision through stochastic control in discrete time and the entire environment is unobserved by the agent in a particular step [13]. We employ an RL-based agent here, which take action to learn a policy for maximizing the reward [13]. The agent takes input of the state of current image status. MDP consists of a set of components, i.e., set of states of the current environment, set of actions to achieve the goal, and the reward to optimize decision strategy. In this paper, the agent’s task is to find a patch from a handwritten page that can be used for writer inspection. The agent will learn the policy through RL to find the highly IdS patches.

In a handwritten page, a text-patch (p) is a $w_p \times w_p$ square box centering at a location l which is encoded with co-ordinate (x, y) . The co-ordinates of the whole page image is ranged between $(0, 0)$ and $(1, 1)$, where the top-left co-ordinate of the page is $(0, 0)$ and bottom-right is $(1, 1)$.

From a patch, we extract some deep neural network-based features. For this, we use the ResNet-50 model [28] which achieved human-like performance on ImageNet data [29], and also met our requirements. Besides, the skip connection concept of ResNet (Residual Network) makes the computation faster compared to some other deep architectures [28], [29],

such as VGG-Net [30]. The ResNet usually takes an input of size 224×224 [28]. For our task also, we chose the w_p equal to 224. In Fig. 3, f_g is a ResNet-50 up to the "avg pool" layer [28], which produces a 2048-dimensional feature vector g . At timestep t , $g_t = f_g(p_t)$.

The feature g_t is then fed into the core network f_h which is basically an RNN (Recurrent Neural Network). We choose the RNN here, since it can memorize the prior patch information. Such memorization is crucial due to its impact on the current time step to find the next patch. The basic RNN unit, employed here is GRU (Gated Recurrent Unit) [31] instead of LSTM (Long Short-Term Memory) due to its simplicity with similar performance gain for our task. GRU also attains lower computational cost since it has only 1 internal state, and 2 gates with fewer parameters, whereas LSTM has 2 internal states and 3 gates with more parameters. Our core network f_h consists of 512 GRU units. The current hidden state h_t of RNN at timestep t is a function of ResNet-produced feature g_t and previous state h_{t-1} . It can be written using GRU gates as follows.

$$\begin{aligned} h_t &= f_h(h_{t-1}, g_t) \\ \text{or, } h_t &= \Gamma_u * c_t + (1 - \Gamma_u) * h_{t-1} \end{aligned} \quad (1)$$

where, $\Gamma_u = \sigma(\text{linear}(h_{t-1}, g_t))$; $c_t = \tanh(\text{linear}(\Gamma_r * h_{t-1}, g_t))$; $\Gamma_r = \sigma(\text{linear}(h_{t-1}, g_t))$.

Γ_u and Γ_r are two gates of GRU, i.e., *update* and *relevant* gates, respectively. Two types of activation functions, *sigmoid* (σ) and *tanh* are used in GRU. The $\text{linear}(\vartheta)$ represents a linear transformation of a vector ϑ ; i.e., $\text{linear}(\vartheta) = \varpi\vartheta + b$, where, ϖ is a weight matrix and b is a bias vector.

Now, the h_t is embedded to f_i to predict an IdS score with respect to a textual patch. The f_i contains a regression layer to generate a scalar-valued IdS score i_t , i.e., $i_t = f_i(h_t)$; $0 \leq i_t \leq 1$. The concept of linear regression on the top of a deep architecture is adopted here [12]. The mean-squared-error is employed here as a loss function to train f_i , and the gradient is backpropagated through f_h and f_g . The IdS score i_t is used

latter for reward shaping during RL.

The h_t is also fed to f_l for obtaining the next patch location l . In f_l , the policy for the location l is decided by a 2-component Gaussian with a fixed variance [32]. The f_l produces the mean of the location policy at time t , and is described as $f_l(h_t) = \text{linear}(h_t)$. Here h_t denotes the state of the core network RNN. The f_l is trained with RL to localize the next patch to focus.

In RL, an agent interacts with the state (s) of an environment and takes action (a) to obtain the reward (r) from the environment [13]. In our task, the reward is generated internally at each time step t instead of any environmental external reward. The state s_t at t takes patch input p_t and summarized into internal state h_t of RNN. The action a_t at t is actually the location-action l_t selected stochastically from a distribution θ_l -parameterized by $f_l(h_t)$ at t . In other words, the *state* is the patches seen so far, and the *action* is (x, y) co-ordinate of the center of the next patch to be looked at.

For *reward* shaping, we propose an internal reward (r_t), generated from the IdS score i_t , as follows.

$$r_t = \begin{cases} i_t & , \text{ if } i_t - i_{t-1} \geq T_{r1} \text{ and } i_t > T_{r2} \\ -(1 - i_t) & , \text{ if } i_t - i_{t-1} < T_{r1} \text{ and } i_t > T_{r2} \\ -i_t & , \text{ otherwise} \end{cases} \quad (2)$$

where, $T_{r1} > 0$ and $T_{r2} > 0$ are two thresholds.

A positive internal reward (r_t) is provided here, if the IdS score (i_t) at current timestep t has increased sufficiently from the score (i_{t-1}) of previous timestep $t - 1$. For all other cases, we penalize the agent by providing a negative internal reward. For our task, $T_{r1} = 0.1$ and $T_{r2} = 0.5$ works well, that are set empirically.

An agent, in RL, entails to learn a stochastic policy $\pi_\theta(l_t|s_{1:t})$ with parameter θ at each timestep t , that maps the past trajectory of environmental interactions $s_{1:t} = p_1, l_1, \dots, p_{t-1}, l_{t-1}, p_t$ to an action distribution l_t . In our task, the policy π_θ is defined by the previously mentioned core network RNN, and s_t is summarized by the state of h_t . For the parametrized policy π_θ , the parameter θ is provided by the parameters θ_g and θ_h of the networks f_g and f_h , respectively, i.e., $\theta = \{\theta_g, \theta_h\}$. The agent learns parameter θ to find an optimal policy that maximizes the expected sum of discounted rewards (r). The cost function becomes as follows.

$$J(\theta) = \mathbb{E}_{\rho(s_{1:T}; \theta)} \left[\sum_{t=1}^T \gamma^{t-1} r_t \right] = \mathbb{E}_{\rho(s_{1:T}; \theta)} [R] \quad (3)$$

where, the transition probability ρ from a state to another, depending on policy π_θ is specified as follows.

$$\rho(s_{1:T}; \theta) = \prod_{t=1}^T \rho(s_{t+1}|s_t, l_t) \pi_\theta(l_t|s_t) \quad (4)$$

where, T is the total count of time-step in an episode and γ is a discounted factor.

Now, we find the optimal policy π^* by optimizing the function parameter θ . The optimal parameter θ^* is defined as $\theta^* = \arg \max_{\theta} J(\theta)$. For finding the optimal policy, gradient ascent is used on policy parameters. Here, we borrow strategies

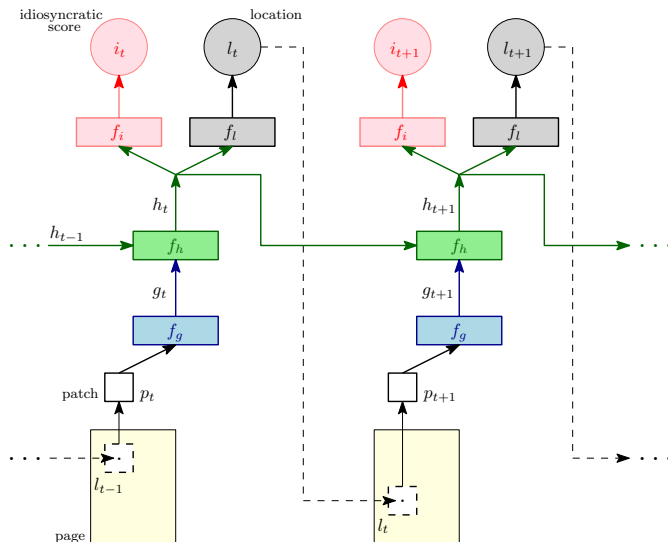


Fig. 3: Idiosyncratic patch detection.

from the RL literature [33] as follows.

$$\begin{aligned} \nabla_{\theta} J(\theta) &= \sum_{t=1}^T \mathbb{E}_{\rho(s_{1:T}; \theta)} [R \nabla_{\theta} \log \pi_{\theta}(l_t | s_t)] \\ &\approx \frac{1}{N} \sum_{n=1}^N \sum_{t=1}^T R^{(n)} \nabla_{\theta} \log \pi_{\theta}(l_t^{(n)} | s_t^{(n)}) \end{aligned} \quad (5)$$

where, $s^{(n)}$'s are trajectories obtained by executing the agent on policy π_{θ} for $n = 1, 2, \dots, N$ episodes. The gradient estimator does not depend on transition probability ρ . Moreover, the $\nabla_{\theta} \log \pi_{\theta}(l_t | s_t)$ part can be computed from the gradient of RNN with standard backpropagation [34].

The gradient estimator may suffer from high variance, therefore, variance reduction is necessary [35]. The variance reduction with baseline (b) can be employed here to understand whether a reward is better than the expected one. Now, the gradient estimator takes the following form.

$$\nabla_{\theta} J(\theta) \approx \frac{1}{N} \sum_{n=1}^N \sum_{t=1}^T (R_t^{(n)} - b_t) \nabla_{\theta} \log \pi_{\theta}(l_t^{(n)} | s_t^{(n)}) \quad (6)$$

where, $R_t = Q^{\pi_{\theta}}(s_t, l_t) = \mathbb{E} \left[\sum_{t \geq 1} \gamma^{t-1} r_t | s_t, l_t, \pi_{\theta} \right]$ and $b_t = V^{\pi_{\theta}}(s_t) = \mathbb{E} \left[\sum_{t \geq 1} \gamma^{t-1} r_t | s_t, \pi_{\theta} \right]$ are known as *Q-value function* and *value function*, respectively [35]. The *Q-value function* follows the execution of action l_t , but the *value function* does not depend on l_t . We learn the baseline by reducing the squared error between *Q-value function* and *value function*.

In this paper, we adopt the idea of finding the next location through the recurrent neural network from [32]. However, our architecture of Fig. 3 is quite new, where the f_g, f_h, f_i nets are different from [32]. The proposed internal reward-generating technique induced by IdS score is also a new contribution.

From the architecture of Fig. 3, we obtain top-scoring k number of idiosyncratic (IdS) patches. Therefore, the number of timesteps (T) in an episode equals to k . We also empirically fix the number of episodes (N) as 1000.

IV. WRITER IDENTIFICATION

From a handwritten page sample, we obtained k number of highly IdS patches (p_j ; for $j = 1, 2, \dots, k$) that are used for writer identification (WI). Adak et al. [6] showed promising outcomes from auto-derived features compared to handcrafted features while dealing with intra-variable writing. Therefore, in this paper, we focus on obtaining auto-derived deep features. Moreover, in [6], the authors performed an empirical study with several state-of-the-art deep neural nets and obtained the best performance using Xception net [36]. The contemporary Inception-ResNet-v2 architecture works better than Xception net and Inception-v4 [36], [37] on ILSVRC database [29]. Therefore, we adopt the Inception-ResNet-v2 [37] for deep feature extraction only, from a handwritten text patch. The rest of the writer-inspection architecture is our proposal.

The size of an obtained patch p_j is 224×224 . We also attained the center location l_j (south-east co-ordinate among four central locations) corresponding to each p_j . From p_j , we obtain p'_j of size 299×299 , by a padding of the proper

width. The west and north sided padding widths are of size $\lfloor (299 - 224)/2 \rfloor = 37$ each, whereas the east and south sided are of $\lceil (299 - 224)/2 \rceil = 38$. The padded region is filled with the original intensity values of the input image. We generate p'_j to employ some earlier layers of Inception-ResNet-v2 architecture that usually takes input of size 299×299 . We use up to the "average pooling" [37] layer of Inception-ResNet-v2 as a feature extractor and refer to it as "I-net" in the rest of this paper. Therefore, I-net produces a 1536-dimensional feature vector [37].

Now, we discuss the architecture for WI as shown in Fig. 4. The last layer of the I-net is the "average pooling" [37] layer of Inception-ResNet-v2. After this layer, we use a dropout [38] of 20% neurons to reduce over-fitting. Next, we add a fully connected (FC) layer to obtain a feature vector of size d from each patch. Then this feature vector is transferred through a *softmax* activation function. Each patch p'_j produces a softmax probability distribution $s_j^{(d)}$; $\forall j = 1, 2, \dots, k$, over class labels. $\sum_d s_j^{(d)} = 1$. Here, k is the number of patches obtained from a page, and d is the total number of classes, i.e., the total count of writers in a database. Now, all $s_j^{(d)}$'s obtained from p'_j 's are combined to obtain the *writer_id* of a page, as follows.

$$writer_id = \arg \max_d z^{(d)} \quad (7)$$

where, $z^{(d)} = \frac{\sum_{j=1}^k w_j s_j^{(d)}}{\sum_{j=1}^k w_j}$, and $\sum_d z^{(d)} = 1$. Here, $z^{(d)}$ is the weighted arithmetic mean of $s_j^{(d)}$'s. A weight w_j is associated with $s_j^{(d)}$, which is determined from the IdS score i_j of a patch p_j as follows.

$$w_j = \begin{cases} \alpha_w i_j & , \text{ if } i_j > 0.1 \\ 1 & , \text{ otherwise} \end{cases} \quad (8)$$

where, α_w is a scalar multiplier, empirically set to 10.

We use cross-entropy [39] as the loss function because of its good performance in multi-class classification. The regularization [39] is also used here to reduce the overfitting problem. The SGD (Stochastic Gradient Descent) with momentum is employed to optimize the cost function [39].

V. WRITER VERIFICATION

In case of writer verification (WV), we authenticate an unknown handwritten sample based on the samples of a known writer-database. Therefore, here the task is to take input of two writing samples and produce the output either "*same*" if they are written by the same writer, or "*different*" otherwise [3]. To measure the similarity between handwritten pages, we extract the page-level feature vectors corresponding to these pages, and compare between the feature vectors.

The auto-derived deep features are also used here since such features outperformed the handcrafted features [6]. Similar to the case of WI, at first, we extract q ($= 1536$)-dimensional deep feature vectors ($v^{(j)} : \{v_1^j, v_2^j, \dots, v_q^j\}$; $\forall j = 1, 2, \dots, k$) from each of the top k IdS patches (p'_j) using I-net (refer to Fig. 5). Now, all the feature vectors $v^{(j)}$'s obtained from all the patches p'_j 's are aggregated to obtain a single q -dimensional feature vector ($v^{(\mu)} : \{v_1^{\mu}, v_2^{\mu}, \dots, v_q^{\mu}\}$) corresponding to a

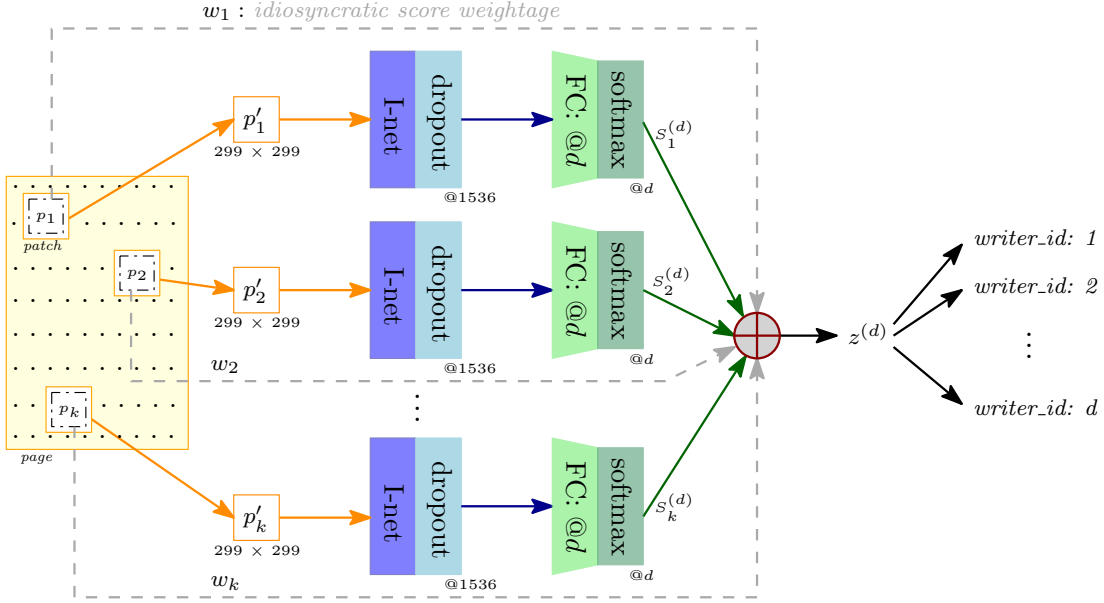


Fig. 4: Writer identification architecture.

handwritten page sample (H). The $v^{(\mu)}$ is calculated as follows. $v^{(\mu)} : \{v_1^\mu = \frac{1}{k} \sum_{j=1}^k v_1^j, v_2^\mu = \frac{1}{k} \sum_{j=1}^k v_2^j, \dots, v_q^\mu = \frac{1}{k} \sum_{j=1}^k v_q^j\}$. We present this method of generating a *Mean Aggregated Feature* (MAF) from multiple text-patches of a page in Algorithm 1: MAF (refer to Appendix A of the supplementary material). Our MAF algorithm is different from the page-level feature generation using *Strategy-Mean* of [6].

We propose another *max Aggregated Feature* (XAF) generation from multiple patches of a page in Algorithm 2: XAF (refer to Appendix A of the supplementary material). The aggregated feature $v^{(\mu)}$ is calculated as follows. $v^{(\mu)} : \{v_1^\mu = \max(v_1^1, v_1^2, \dots, v_1^k), v_2^\mu = \max(v_2^1, v_2^2, \dots, v_2^k), \dots, v_q^\mu = \max(v_q^1, v_q^2, \dots, v_q^k)\}$. Our XAF algorithm is also different from *Strategy-Major* of [6] for page-level feature generation.

Thus, we have obtained a feature-vector $v^{(\mu)}$ from a handwritten page (H). For WV, we need to examine the writing style similarity/dissimilarity between pages. In other words, we measure the similarities among feature-vectors $v^{(\mu)}$'s representing pages H 's. For similarity metric learning, we adopt the idea of triplet network [40], which is quite a popular technique in the literature [40]–[42]. In the triplet net (refer to Fig. 6), three identical neural nets (NN's) produce three feature vectors $v_A^{(\mu)}, v_P^{(\mu)}, v_N^{(\mu)}$ in parallel from three handwritten pages H_A, H_P, H_N , respectively, i.e., $v_A^{(\mu)} = NN(H_A)$, $v_P^{(\mu)} = NN(H_P)$, $v_N^{(\mu)} = NN(H_N)$. The three NN's share weights among them.

In the triplet network, we compare a positive sample (H_P) and a negative sample (H_N) with reference to an anchor/baseline sample (H_A), simultaneously. H_A and H_P handwritten samples are written by the same writer, whereas H_A and H_N samples are written by two different writers. We use Euclidean distance (D) between $v_A^{(\mu)}$ and $v_P^{(\mu)}$ as a distance metric to compare H_A and H_P , i.e., $D(H_A, H_P) = \|v_A^{(\mu)} - v_P^{(\mu)}\|_2$. Similarly, we compare H_A and H_N with $D(H_A, H_N) = \|v_A^{(\mu)} - v_N^{(\mu)}\|_2$. Finally, the wings of the

triplet network are joined using a loss function, called triplet loss (\mathcal{L}) [41] to train with the similarity/dissimilarity metric. This \mathcal{L} is defined as follows.

$$\mathcal{L}(H_A, H_P, H_N) = \max(D(H_A, H_P) - D(H_A, H_N) + \alpha_m, 0) \quad (9)$$

where, α_m is a margin parameter. Empirically, α_m is set as 0.2, when checked in the interval $[0.1, 0.9]$ with a step of 0.1. This triplet loss ensures the positive sample to be closer to the anchor than that of the negative one, by at least a margin α_m .

The overall cost function (\mathcal{J}) of the triplet network is the sum of individual losses on different triplets, over the training set cardinality M , which is given as follows.

$$\mathcal{J} = \sum_{m=1}^M \mathcal{L}(H_A^{(m)}, H_P^{(m)}, H_N^{(m)}) \quad (10)$$

Here, with reference to an anchor sample (H_A), we choose the hardest positive sample (H_P) and the hardest negative sample (H_N) within a mini-batch to form a triplet [42]. This hard-triplet is hard to train, which increases the computational efficiency of the learning algorithm. The SGD with momentum is employed here for minimizing \mathcal{J} .

In [6], a Siamese net with the contrastive loss [43] is used for WV. In this paper, we utilize a triplet loss-based network, since it works better than the contrastive loss-based Siamese net [41]–[43].

All handwritten page pairs (H_i, H_j) scribbled by the *same* writer are represented by \mathcal{P}_{same} , and all writing sample pairs of different writers are denoted as \mathcal{P}_{diff} . For system performance evaluation, we define a set of true positives (TP) at a threshold t_d , when all writing sample pairs are correctly classified as "same", i.e.,

$$TP(t_d) = \{(H_i, H_j) \in \mathcal{P}_{same}, \text{ with } D(H_i, H_j) \leq t_d\} \quad (11)$$

Similarly, a set of true negatives (TN) at t_d is defined where

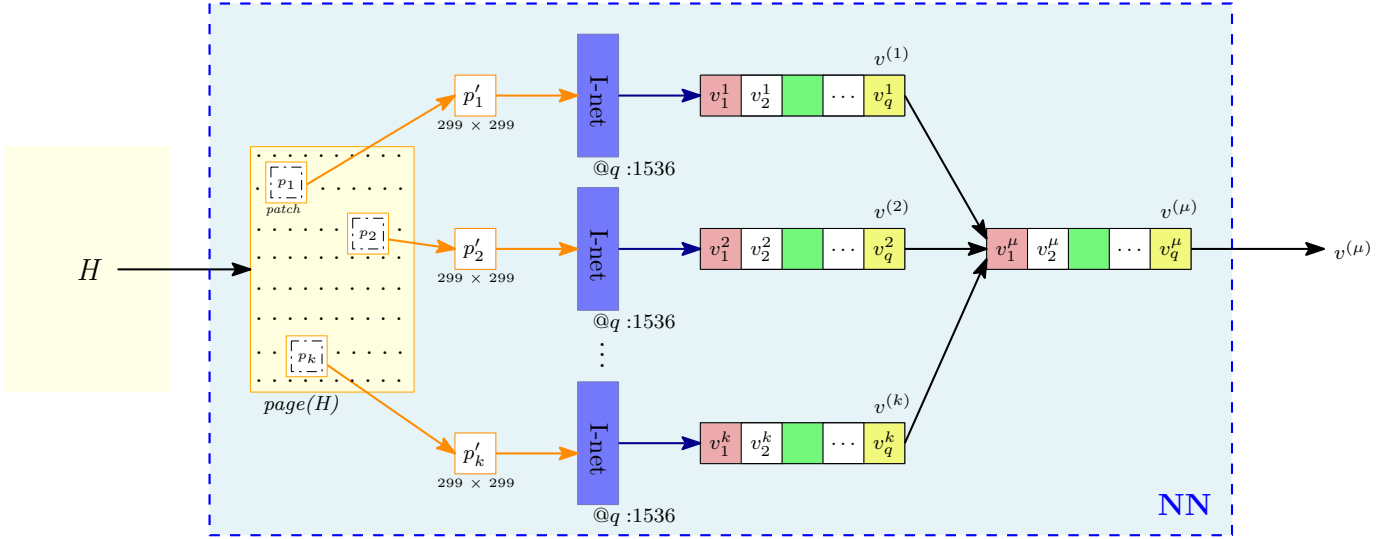


Fig. 5: Feature extraction for writer verification.

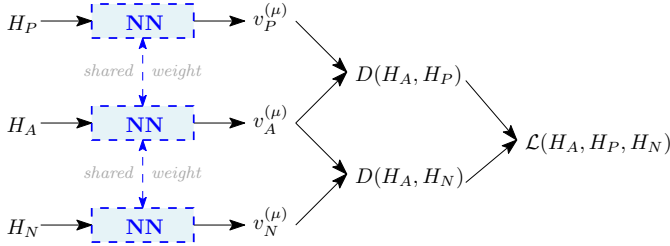


Fig. 6: Triplet Network (refer to Fig. 5 for NN).

all pairs are correctly classified as "different", i.e.,

$$TN(t_d) = \{(H_i, H_j) \in \mathcal{P}_{diff}, \text{ with } D(H_i, H_j) > t_d\} \quad (12)$$

The true positive rate (TPR) and true negative rate (TNR) for a given writing distance t_d are defined below.

$$TPR(t_d) = \frac{|TP(t_d)|}{|\mathcal{P}_{same}|}; \quad TNR(t_d) = \frac{|TN(t_d)|}{|\mathcal{P}_{diff}|} \quad (13)$$

The overall *accuracy* (balanced) [44] for WV is calculated as follows.

$$Accuracy = \max_{t_d \in D} \frac{TPR(t_d) + TNR(t_d)}{2} \quad (14)$$

where, t_d varies with a step of 0.1 in the range of D .

VI. EXPERIMENTS AND DISCUSSIONS

In this section, we discuss the experiments performed to evaluate our proposed system. We analyzed the system performance based on idiosyncratic patch detection, writer identification (WI), and writer verification (WV). We also compared the proposed approach with some past methods. Before proceeding to the experimental analysis, we first present the database employed for our experiments.

A. Database Employed

For experimental analysis, we required a database (DB) containing intra-variable handwritten pages of a writer. As far

as we know, in the literature, except [6], no database contains such intra-variable handwritten samples. Therefore, we only used the two databases of [6], namely *controlled* (D_c) and *uncontrolled* (D_{uc}) datasets which are briefly discussed below.

1) *Controlled* (D_c): This database comprises a total of 600 Bengali handwritten pages written by 100 writers, i.e., 6 pages per writer. This database contains 3 sets (S_f, S_m, S_s) of intra-variable writing based on various speeds of writing (*fast, medium, slow*). Each of these 3 sets has 2 handwritten pages per writer. For example, a writer's handwritten sample of S_f set varies extensively with his/her writing sample of S_s .

D_c was generated in a controlled way, where the writers were aware of the experimentation and were asked to write at different speeds, e.g., normal/medium, faster than normal, and slower than normal. To validate the writing speed (v_w), the writing time (τ) of a page was noted. The total stroke-length (ℓ) of a page was also computed [6]. Now, $v_w = \ell/\tau$. The decision to place a handwritten page into one of the subsets S_f, S_m, S_s was taken based on v_w with respect to two data-driven thresholds. More details on D_c can be found in [6].

2) *Uncontrolled* (D_{uc}): Similar to D_c , this database contains 600 Bengali handwritten pages of 100 individuals, where each writer wrote 6 pages. However, the D_c and D_{uc} datasets are writer-disjoint. Here too, the database is divided into 3 sets (S_f, S_m, S_s) of intra-variable writing, where each set comprises 2 pages per writer.

The D_{uc} was created in an uncontrolled manner, where the writers were not informed of the experimentation before their scribbling. For this, a real school examination was conducted. In the answer sheets, intra-variation was observed due to the writing speed, and some behavioral/psychological aspects [45] such as anxiety, stress to recall answers, nervousness to complete, the panic of low marks, etc. The handwritten pages were grouped into S_f, S_m, S_s sets using a deep feature-based clustering technique followed by validation of handwriting experts. An elaborate discussion on D_{uc} is reported in [6].

The data of D_c and D_{uc} were augmented to reduce the overfitting problem. In data augmentation, the *offline Drop-*

Stroke [6] technique was used, where some writing-strokes were dropped randomly without creating any extra stroke components. A graph-based strategy was used here to obtain the strokes. A method as given in [46], [47] that generates duplicate offline synthetic signatures using some cognitive-inspired algorithm, may be an alternative data augmentation technique, but a costly process for producing full-page writing instead of a signature.

For data augmentation [6], a full handwritten page was roughly split horizontally into two halves [17]. Then on each half, the *offline DropStroke* was used to generate 10 augmented samples. Therefore, a full page generated 22 ($= 2 \times (1 + 10)$) samples. Now, each of the sets S_f , S_m , S_s of D_c and S_f , S_m , S_s of D_{uc} contained 2 full pages per writer, therefore, each of them generated 44 ($= 2 \times 22$) samples from each of the 100 individuals. Each of these samples was input to our system.

In this paper, the experimental setup was similar to that in [6]. Both the databases D_c and D_{uc} were divided into training, validation, and test set in the ratio of 2 : 1 : 1. For example, S_f set was divided into S_{f1} (training), S_{f2} (validation), and S_{f3} (test) subsets, which contained 22, 11, and 11 handwriting samples from each of the 100 writers. Actually, S_{f1} contained samples obtained from the first full page of S_f , whereas, S_{f2} and S_{f3} comprised samples acquired from top and bottom halves of the second page of S_f , respectively. As a matter of fact, $S_f = S_{f1} \cup S_{f2} \cup S_{f3}$. Similarly, $S_m = S_{m1} \cup S_{m2} \cup S_{m3}$, $S_s = S_{s1} \cup S_{s2} \cup S_{s3}$, $S'_f = S'_{f1} \cup S'_{f2} \cup S'_{f3}$, $S'_m = S'_{m1} \cup S'_{m2} \cup S'_{m3}$, and $S'_s = S'_{s1} \cup S'_{s2} \cup S'_{s3}$.

B. Performance of Idiosyncratic Patch Detection

In this subsection, we analyze the performance of our system for detecting idiosyncratic (IdS) patches.

As mentioned in Section III-A, the handwriting experts were given multiple patches for ground-truthing. The patches were obtained by sliding a 224×224 sized window horizontally through the text-lines with a stride of 96, fixed empirically. Furthermore, the experts were shown a full page of handwriting on which they pointed to some patches randomly and put their opinion scores. The experts provided their scores independently without knowing the scores provided by others.

The proposed system predicted the IdS opinion score of a detected patch through deep regression analysis. Therefore, we used a standard performance measure for prediction, i.e., MAE (Mean Absolute Error). MAE is the arithmetic mean of the absolute differences between actual and predicted IdS opinion scores of the patches. The actual IdS score was obtained by averaging the scores of those patches with whom the IoU (Intersection over Union) [48] measures of the predicted patch were greater than 0.5. The employed training, validation, and test sets are discussed in the previous subsection. Some hyper-parameters were also tuned here.

In TABLE I, we present the MAE results when k number of patches were chosen from each text sample. The results obtained from both D_c and D_{uc} databases are shown here. For $k = 125$, we obtained the lowest MAE of 1.03% and 1.67% for D_c and D_{uc} , respectively.

MAE focused on measuring the correctness of predicting the IdS score and did not guarantee to infer a *highly* IdS opinion

TABLE I: Performance of idiosyncratic patch detection

| # patches (k) | Mean Absolute Error (MAE) % | | Mean Idiosyncratic Score (MIS) | |
|----------------------|--------------------------------|-------------|-----------------------------------|--------------|
| | D_c | D_{uc} | D_c | D_{uc} |
| 50 | 2.08 | 2.96 | 0.618 | 0.610 |
| 75 | 1.77 | 1.97 | 0.774 | 0.761 |
| 100 | 1.30 | 2.08 | 0.879 | 0.868 |
| 125 | 1.03 | 1.67 | 0.832 | 0.826 |
| 150 | 1.75 | 1.86 | 0.783 | 0.779 |
| 175 | 2.14 | 2.02 | 0.658 | 0.651 |
| 200 | 2.85 | 2.98 | 0.595 | 0.593 |

score. However, in this research, we were interested in highly IdS patches for writer inspection. Therefore, it was necessary to propose some measure which focused on analyzing highly IdS opinion score.

At this point, we proposed a performance measure, which was the arithmetic mean of normalized IdS opinion scores of k number of patches, which were obtained from each text sample. This Mean Idiosyncratic Score (MIS) inferred the detection of highly IdS patches, when the MIS was high. As shown in TABLE I, we obtained the highest MIS of 0.879 and 0.868 for D_c and D_{uc} , respectively, when $k = 100$. However, the MIS did not guarantee the correct prediction of an IdS score. Therefore, to analyze the correctly-predicted highly IdS patch, we intended to observe both the MAE and MIS. From TABLE I, we can see that $k = 125$ produced the lowest MAE, whereas $k = 100$ produced the highest MIS. Therefore, we checked the writer-inspection performance by varying the value of k in the following subsections.

C. Performance of Writer Identification

In this and next subsections, we present the WI and WV performances of the proposed system. Our system was evaluated with the same experimental strategy of [6].

For WI/WV, a 9-tuple accuracy measure obtained from various experimental setups was used in [6]. However, in this 9-tuple, 3 elements computed the actual system performance for intra-variable handwriting inspection, i.e., training/testing on highly disparate writing styles, which was termed as *3-tuple accuracy*. Therefore, in this paper, we focused on this 3-tuple accuracy measure to evaluate WI/WV performance. The 3-tuple accuracy was (AE_{smv} , AE_{sfv} , AE_{mfv}). AE_{smv} was the average accuracy obtained from experimental setups E_{sm} and E_{ms} . In E_{sm} setup, the training was performed on S_{s1} and testing was done on S_{m3} , i.e., S_{s1}/S_{m3} , while employing D_c . The E_{ms} was the reverse experimental setup, i.e., S_{m1}/S_{s3} , when using D_c . As a matter of fact, on D_{uc} , E_{sm} was S_{s1}/S_{m3} , and E_{ms} was S_{m1}/S_{s3} . Similarly, AE_{sfv} and AE_{mfv} were obtained. A more detailed discussion on the experimental setup can be found in [6].

During the training of our system, some hyper-parameters were tuned and fixed. We fixed momentum = 0.9, learning rate = 0.01, weight decay = 10^{-4} and epoch = 1000.

For WI, the standard Top-N criterion was chosen, where we computed Top-1, Top-2, and Top-5 accuracy measure [6]. As mentioned earlier, the WI task can be seen as a multi-class classification problem and we present the results in terms of accuracy.

TABLE II: Top-1 writer identification performance

| DB | # patches (k) | 3-tuple accuracy (%) | | |
|----------|----------------------|----------------------|--------------|--------------|
| | | AE_{smv} | AE_{sfv} | AE_{mfv} |
| D_c | 75 | 81.72 | 74.83 | 77.92 |
| | 100 | 88.37 | 81.57 | 84.51 |
| | 125 | 87.75 | 81.21 | 83.83 |
| | 150 | 84.58 | 77.16 | 80.53 |
| D_{uc} | 75 | 81.95 | 74.49 | 78.13 |
| | 100 | 87.25 | 79.67 | 82.61 |
| | 125 | 86.74 | 79.69 | 82.53 |
| | 150 | 82.86 | 76.15 | 78.64 |

TABLE III: Top-N writer identification with $k = 100$

| DB | Top-N | 3-tuple accuracy (%) | | |
|----------|-------|----------------------|------------|------------|
| | | AE_{smv} | AE_{sfv} | AE_{mfv} |
| D_c | Top-1 | 88.37 | 81.57 | 84.51 |
| | Top-2 | 88.63 | 81.84 | 85.01 |
| | Top-5 | 91.54 | 84.28 | 87.18 |
| D_{uc} | Top-1 | 87.25 | 79.67 | 82.61 |
| | Top-2 | 88.13 | 80.81 | 83.33 |
| | Top-5 | 91.08 | 83.65 | 87.10 |

In TABLE II, we present the Top-1 WI performance in terms of 3-tuple accuracy using Inception-ResNet-v2 [37] as I-net. From TABLE I, we noticed the lowest MAE and the highest MIS were obtained for $k = 125$ and $k = 100$, respectively. Therefore, here we varied the k in a smaller span from 75 to 150 with a step of 25. Overall, we obtained the best performance for $k = 100$ on both databases D_c and D_{uc} . For $k = 125$, the overall performance was the second-best, which was very close to the best. In general, the best 3-tuple accuracies for D_c and D_{uc} databases were (88.37%, 81.57%, 84.51%) and (87.25%, 79.67%, 82.61%), respectively. On D_{uc} , the accuracy AE_{sfv} was slightly better for $k = 125$ than for $k = 100$. Overall, the intra-variable WI performance on D_c was better than D_{uc} .

In general, our WI system performed the best when 100 patches were selected from a text sample. Therefore, in this paper, we fix $k = 100$, for presenting the rest of the experiments on intra-variable WI.

In TABLE III, we present Top-1, Top-2, and Top-5 WI performances for $k = 100$ with Inception-ResNet-v2 as I-net. The Top-2 measure was very close to the Top-1 performance. On D_c and D_{uc} databases, the Top-5 3-tuple accuracies were (91.54%, 84.28%, 87.18%) and (91.08%, 83.65%, 87.10%), respectively.

Our WI architecture (refer to Fig. 4) is quite generalized, where we can employ various deep-feature generators as I-net. Apart from using the front part of the Inception-ResNet-v2 as I-net, we checked with the front part (up to "average pooling" layer) of some other powerful deep architectures, e.g., Inception-v4 [37], Xception net [36], as I-net. In TABLE IV, we present the Top-1 WI performance with various I-nets when $k = 100$. Overall, we attained the best 3-tuple accuracies of (88.37%, 81.57%, 84.51%) and (87.25%, 79.67%, 82.61%) on D_c and D_{uc} databases, respectively, by employing Inception-ResNet-v2. The Inception-v4 performed similarly well, and became overall the second-best. The Xception net also performed quite well, though secured the last rank. The Xception net performed better than some state-of-the-art deep neural nets, e.g., Inception v3, Inception v2, GoogLeNet (Inception v1), VGG-16, ResNet-101, SqueezeNet, etc. [4], [6], [36].

TABLE IV: Top-1 writer identification on $k = 100$ with various I-nets

| DB | I-net | 3-tuple accuracy (%) | | |
|----------|--------------------------|----------------------|--------------|--------------|
| | | AE_{smv} | AE_{sfv} | AE_{mfv} |
| D_c | Inception-ResNet-v2 [37] | 88.37 | 81.57 | 84.51 |
| | Inception-v4 [37] | 88.20 | 81.53 | 84.52 |
| | Xception net [36] | 87.76 | 80.72 | 83.96 |
| D_{uc} | Inception-ResNet-v2 [37] | 87.25 | 79.67 | 82.61 |
| | Inception-v4 [37] | 87.21 | 79.71 | 82.53 |
| | Xception net [36] | 86.41 | 79.06 | 82.00 |

D. Performance of Writer Verification

Here also, we used the 3-tuple accuracy measure obtained from a similar experimental setup for WI of the previous subsection. The tuning of hyper-parameters was also similar to the WI. A small difference lies in measuring the accuracy, which has been discussed in Section V.

As mentioned earlier, WV can be perceived as a binary classification task to decide two handwriting samples either as "same" or "different" based on a given text sample. We present the results here in terms of accuracy (balanced), as given in Section V.

For WV, the features obtained from the patches of a text sample was aggregated using two different algorithms, i.e., MAF (Mean Aggregated Feature) and XAF (maX Aggregated Feature). We compare these two algorithms in TABLE V, where we present the 3-tuple accuracy for WV on a variable number of patches (k) on databases D_c and D_{uc} . Inception-ResNet-v2 was used here as I-net, and the triplet network was used for similarity learning.

From TABLE V, we note that overall we obtained the best performance for $k = 100$ using both MAF and XAF algorithms on D_c and D_{uc} . Therefore, in this paper, we used $k = 100$ for presenting the rest of the experiments for intra-variable WV. Comparing MAF and XAF, we observed that MAF worked better than XAF on a variable number of patches for both the databases D_c and D_{uc} . On D_c and D_{uc} , the overall best 3-tuple accuracies were (94.87%, 86.78%, 92.12%) and (92.45%, 86.35%, 90.97%) using MAF, while $k = 100$. In general, the intra-variable WV performance on D_c was better than D_{uc} .

Similar to TABLE IV for WI, here in TABLE VI, we present the WV performance with various I-nets by employing

TABLE V: Writer verification performance

| DB | Algo | # patches (k) | 3-tuple accuracy (%) | | |
|----------|------|----------------------|----------------------|--------------|--------------|
| | | | AE_{smv} | AE_{sfv} | AE_{mfv} |
| D_c | MAF | 75 | 88.24 | 80.63 | 85.88 |
| | | 100 | 94.87 | 86.78 | 92.12 |
| | | 125 | 94.62 | 86.32 | 91.52 |
| | | 150 | 92.83 | 84.18 | 89.01 |
| | XAF | 75 | 83.76 | 75.59 | 81.72 |
| | | 100 | 90.71 | 82.47 | 87.93 |
| 125 | | 90.49 | 82.21 | 87.18 | |
| D_{uc} | MAF | 75 | 84.59 | 79.00 | 83.09 |
| | | 100 | 92.45 | 86.35 | 90.97 |
| | | 125 | 91.76 | 86.43 | 90.63 |
| | XAF | 150 | 90.63 | 85.25 | 89.20 |
| | | 75 | 81.78 | 75.40 | 80.19 |
| | | 100 | 88.23 | 81.86 | 86.46 |
| | | 125 | 88.05 | 81.34 | 86.17 |
| | | 150 | 85.36 | 79.33 | 83.91 |

TABLE VI: Writer verification with various I-nets

| DB | I-net | 3-tuple accuracy (%) | | |
|----------|--------------------------|----------------------|--------------|--------------|
| | | AE_{smv} | AE_{sfv} | AE_{mfv} |
| D_c | Inception-ResNet-v2 [37] | 94.87 | 86.78 | 92.12 |
| | Inception-v4 [37] | 94.71 | 86.34 | 91.83 |
| | Xception [36] | 93.66 | 85.19 | 90.05 |
| D_{uc} | Inception-ResNet-v2 [37] | 92.45 | 86.35 | 90.97 |
| | Inception-v4 [37] | 91.86 | 86.02 | 90.63 |
| | Xception [36] | 90.39 | 84.06 | 89.17 |

TABLE VII: Writer verification with various similarity learning

| DB | Similarity learning | 3-tuple accuracy (%) | | |
|----------|---------------------|----------------------|--------------|--------------|
| | | AE_{smv} | AE_{sfv} | AE_{mfv} |
| D_c | Triplet net [40] | 94.87 | 86.78 | 92.12 |
| | Siamese net [43] | 88.95 | 81.59 | 86.78 |
| D_{uc} | Triplet net [40] | 92.45 | 86.35 | 90.97 |
| | Siamese net [43] | 87.40 | 80.63 | 84.46 |

MAF, triplet net and $k = 100$. We obtained here the best 3-tuple accuracy (94.87%, 86.78%, 92.12%) and (92.45%, 86.35%, 90.97%) using Inception-ResNet-v2 on D_c and D_{uc} , respectively. The results, employing Inception-v4 were very close to the best performance.

In TABLE VII, we present the WV performance with various similarity learning using MAF, Inception-ResNet-v2, and $k = 100$. The triplet network worked better than the Siamese net, and produced 3-tuple accuracies of (94.87%, 86.78%, 92.12%) and (92.45%, 86.35%, 90.97%) on D_c and D_{uc} , respectively.

From the above experiments on writer inspection, our major observations are summarized as follows.

(i) The WI/WV performance on D_c database was better than on D_{uc} .

(ii) For WI/WV, the overall best performance was obtained while 100 ($= k$) IdS patches per text sample were used.

(iii) For WI/WV, the front part of the Inception-ResNet-v2 (up to "average pooling" layer) worked the best as I-net.

(iv) Overall, the WI/WV performances in terms of individual elements of 3-tuple accuracy in decreasing order were as follows: $AE_{smv} > AE_{mfv} > AE_{sfv}$.

(v) For WV, in general, the MAF algorithm worked better than XAF.

(vi) For WV, the triplet network worked better than the Siamese net for similarity learning.

E. Comparison

In this subsection, we compare our method with some major related work reported in the literature. We first compare with respect to idiosyncrasy analysis, then WI followed by WV.

1) *Comparison of Idiosyncrasy Analysis*: To compare our method of idiosyncrasy analysis, we came across only one work [11] reported in the literature.

In this paper, our task is to predict the idiosyncratic (IdS) score from a patch using deep regression analysis. Adak et al. [11] modeled the task into classification problem to classify the text-patches into some highly IdS classes, i.e., ID_1 class when normalized score i_j of patch p_j was in the interval (0.9, 1], ID_2 when i_j was in the range (0.8, 0.9], ID_3 when i_j was in (0.7, 0.8], and so on. For comparison purposes, we did a similar setting here, i.e., if i_j lied in (0.9, 1], then p_j was

TABLE VIII: Comparison of idiosyncrasy analysis

| DB | Method | Accuracy (%) |
|----------|------------------|--------------|
| D_c | Adak et al. [11] | 90.56 |
| | Proposed | 98.35 |
| D_{uc} | Adak et al. [11] | 89.85 |
| | Proposed | 97.74 |

in class ID_1 , and so forth, to be in ID_2 and ID_3 . Here, if the actual score i_j of p_j was in ID_1 , and the regression-based predicted score (\neq actual score) of p_j was also in ID_1 , then the p_j was correctly classified (true positive), where the relaxed error was less than 0.1. For comparison, we calculated the accuracy (balanced) [44] from the top three IdS classes (ID_1 , ID_2 , and ID_3 , i.e., ID_{1-3}), since ID_{1-3} produced the best performance in [11]. The quantitative comparison measure, using 100 patches obtained from each text sample of intra-variable databases (D_c and D_{uc}), is presented in TABLE VIII. From this table, we observe that our proposed method produced 98.35% and 97.74% accuracies on D_c and D_{uc} databases, respectively, which were better than the performances obtained in [11].

2) *Comparison of Writer Identification*: For comparative analysis concerning WI and WV from intra-variable handwriting, we maintained similar experimental setups, employed databases, and performance measures as used in this paper (refer to Section VI-A), which is the same as in [6].

An empirical study on intra-variable writer inspection was presented in [6], where the XceptionNet-based method "XN_allo_mean" performed better than some major state-of-the-art deep feature-based architectures (e.g., SqueezeNet, GoogLeNet, VGG-16, ResNet-101, etc.) and some handcrafted feature-based models. Therefore, from [6], we compared only with the XN_allo_mean method.

Another work reported in [11] was on analyzing IdS handwriting to identify a writer. However, they did not work on intra-variable writing. Therefore, here, we were interested in executing the method of [11] on our intra-variable writing's experimental setup.

The state-of-the-art writer inspection methods did not focus on intra-variable handwriting. However, we intended to see the performance of the past methods on intra-variability. Therefore, we performed a comparative study with the past significant handcrafted [3], [15]–[17] and deep feature-based [6], [11], [23]–[26] methods.

In TABLE IX, we compare our proposed WI model (employing $k = 100$, and Inception-ResNet-v2 as I-net) with some crucial related work in terms of Top-1 3-tuple accuracy on databases D_c and D_{uc} . From this table, we can see that handcrafted feature-based models performed poorly. The SIFT-based architecture [17] performed the best among the handcrafted feature-based models. The deep feature-based methods obtained better results than the handcrafted feature-based models. He et al. [25] identified the writers based on a single word. For comparison, we executed their WI method on every segmented word, and decided the ensemble page-level writer by max-voting. WLE (Word Length Estimation) was chosen here as an auxiliary task. Our proposed model performed the best, which attained (88.37%, 81.57%, 84.51%)

TABLE IX: Comparison of Top-1 writer identification

| DB | Method | 3-tuple accuracy (%) | | |
|----------|--------------------------------|----------------------|--------------|--------------|
| | | AE_{smv} | AE_{sfv} | AE_{mfv} |
| D_c | Macro-micro [15] | 37.81 | 30.47 | 35.63 |
| | Hinge [3] | 46.56 | 39.95 | 44.16 |
| | LBPPruns_G + COLD [16] | 49.13 | 42.66 | 46.47 |
| | SIFT (SDS + SOH) [17] | 52.36 | 45.61 | 48.55 |
| | CaffeNet [26] | 65.74 | 55.36 | 61.11 |
| | CNN + GMM [23] | 66.57 | 56.17 | 61.49 |
| | CNN + Bayesian [24] | 68.29 | 58.35 | 63.24 |
| | Adaptive CNN + WLE [25] | 69.72 | 59.53 | 65.06 |
| | XceptionNet (XN_allo_mean) [6] | 73.74 | 64.12 | 68.94 |
| | Idiosyncrasy + SqueezeNet [11] | 75.42 | 66.75 | 71.04 |
| | Proposed | 88.37 | 81.57 | 84.51 |
| D_{uc} | Macro-micro [15] | 37.01 | 29.77 | 33.92 |
| | Hinge [3] | 46.15 | 39.56 | 43.63 |
| | LBPPruns_G + COLD [16] | 49.03 | 42.39 | 46.35 |
| | SIFT (SDS + SOH) [17] | 51.97 | 45.05 | 48.63 |
| | CaffeNet [26] | 64.52 | 53.89 | 59.54 |
| | CNN + GMM [23] | 65.23 | 54.93 | 60.82 |
| | CNN + Bayesian [24] | 67.42 | 57.31 | 62.78 |
| | Adaptive CNN + WLE [25] | 68.86 | 58.92 | 64.53 |
| | XceptionNet (XN_allo_mean) [6] | 72.52 | 62.79 | 66.53 |
| | Idiosyncrasy + SqueezeNet [11] | 73.68 | 64.07 | 68.84 |
| | Proposed | 87.25 | 79.67 | 82.61 |

and (87.25%, 79.67%, 82.61%) 3-tuple accuracies on D_c and D_{uc} , respectively. The method of [11] ranked the second-best by leveraging idiosyncrasy analysis and SqueezeNet. The other past methods did not focus on the idiosyncrasy of writing. This attests to the importance of IdS handwriting analysis for intra-variable writer inspection.

3) *Comparison of Writer Verification*: This subsection compares our proposed WV method with some major state-of-the-art handcrafted [3], [15]–[17] and deep feature-based [6], [11], [23]–[26] techniques, similar to the WI. The experimental setups, employed databases, and performance measures were the same as in [6].

Some of the past methods [11], [16], [17], [23]–[26] did not report working with WV. However, these methods can easily verify a writer by using some distance measure between the features extracted from the known and questioned handwriting samples [3], [6]. Therefore, for a comparative study, we executed these past methods to verify the writer while employing the Euclidean distance measure.

In [6], for WV on intra-variable writing, the XceptionNet-based XN_allo_mean performed better than some past handcrafted and deep feature-based methods. Therefore, from [6], we compared our method with the XN_allo_mean only.

In TABLE X, we present the WV performance of some important past methods executed on databases D_c and D_{uc} . Here also, the deep features worked better than the handcrafted features. Our proposed method obtained the best result, when we used $k = 100$, Inception-ResNet-v2 as I-net, MAF for feature aggregation, and the triplet network for similarity learning. We achieved (94.87%, 86.78%, 92.12%) and (92.45%, 86.35%, 90.97%) 3-tuple accuracies on the D_c and D_{uc} databases, respectively. The method of [11] also attained the second-best intra-variable WV performance.

From this comparative study, we observed that our present method outperformed the past methods for writer inspection on intra-variable data. We also observed that idiosyncrasy analysis aided the WI/WV system to perform better on intra-variable handwriting.

TABLE X: Comparison of writer verification

| DB | Method | 3-tuple accuracy (%) | | |
|----------|--------------------------------|----------------------|--------------|--------------|
| | | AE_{smv} | AE_{sfv} | AE_{mfv} |
| D_c | Macro-micro [15] | 48.50 | 36.58 | 41.43 |
| | Hinge [3] | 55.97 | 47.15 | 51.98 |
| | LBPPruns_G + COLD [16] | 59.62 | 50.86 | 55.34 |
| | SIFT (SDS + SOH) [17] | 61.91 | 53.35 | 58.02 |
| | CaffeNet [26] | 75.74 | 64.75 | 68.95 |
| | CNN + GMM [23] | 77.23 | 66.21 | 70.85 |
| | CNN + Bayesian [24] | 78.07 | 67.18 | 71.46 |
| | Adaptive CNN + WLE [25] | 79.12 | 67.34 | 72.09 |
| | XceptionNet (XN_allo_mean) [6] | 80.79 | 70.02 | 74.98 |
| | Idiosyncrasy + SqueezeNet [11] | 83.45 | 72.97 | 78.74 |
| | Proposed | 94.87 | 86.78 | 92.12 |
| D_{uc} | Macro-micro [15] | 47.96 | 35.76 | 40.26 |
| | Hinge [3] | 55.25 | 46.91 | 51.27 |
| | LBPPruns_G + COLD [16] | 58.85 | 49.26 | 54.63 |
| | SIFT (SDS + SOH) [17] | 61.33 | 52.82 | 57.30 |
| | CaffeNet [26] | 75.36 | 64.07 | 68.75 |
| | CNN + GMM [23] | 76.77 | 65.42 | 70.63 |
| | CNN + Bayesian [24] | 77.89 | 67.00 | 71.08 |
| | Adaptive CNN + WLE [25] | 78.66 | 67.12 | 71.94 |
| | XceptionNet (XN_allo_mean) [6] | 79.84 | 69.80 | 74.76 |
| | Idiosyncrasy + SqueezeNet [11] | 81.82 | 71.35 | 77.26 |
| | Proposed | 92.45 | 86.35 | 90.97 |

F. Ablation Study

In this subsection, we validate the requirement of idiosyncratic (IdS) patch detection for writer inspection. Furthermore, we check the need for RL to find IdS patches. For this, we use the strategy of ablation study [49], where we remove a module to see whether the removal has affected the overall system.

1) *Ablating Idiosyncratic Patch Detection*: For writer inspection, our proposed deep feature-based method, with the top 100 IdS patches obtained using RL, performed better than other deep feature-based methods [6], [23]–[26] that did not employ the idiosyncrasy analysis (refer to Section VI-E).

To check the requirement of highly IdS patches, we execute the following two methods that ablate the RL-based IdS patch detection module from our proposed writer inspection system: (i) *Method-Rand_100* that uses 100 random patches obtained from a handwritten sample, (ii) *Method-All* that employs all patches acquired from a sample. These two methods are compared with our proposed WI/WV method that used 100 highly IdS patches.

In TABLE XI, we present the comparative study where we used similar experimental setups as discussed in Sections VI-C, VI-D. All the WI and WV methods of TABLE XI used Inception-ResNet-v2 as I-net. All the WV methods of this table used MAF for feature aggregation, and a triplet network

TABLE XI: Ablation study: idiosyncratic patch detection

| Writer Inspection | DB | Method | 3-tuple accuracy (%) | | |
|-------------------|----------|----------|----------------------|--------------|--------------|
| | | | AE_{smv} | AE_{sfv} | AE_{mfv} |
| WI | D_c | Rand-100 | 63.53 | 52.54 | 58.33 |
| | | All | 73.97 | 64.23 | 69.19 |
| | | Proposed | 88.37 | 81.57 | 84.51 |
| | D_{uc} | Rand-100 | 61.99 | 50.93 | 56.80 |
| | | All | 72.95 | 63.05 | 66.78 |
| | | Proposed | 87.25 | 79.67 | 82.61 |
| WV | D_c | Rand-100 | 73.60 | 62.02 | 66.01 |
| | | All | 80.73 | 70.32 | 75.30 |
| | | Proposed | 94.87 | 86.78 | 92.12 |
| | D_{uc} | Rand-100 | 72.52 | 61.64 | 66.63 |
| | | All | 79.83 | 69.93 | 74.79 |
| | | Proposed | 92.45 | 86.35 | 90.97 |

for similarity learning. We repeated the experiment of *Method-Rand_100* 30 times, and present the average result in this table. From TABLE XI, we can observe that our proposed method (with top 100 IdS patches) outperformed the *Method-Rand_100* (using 100 random patches) and *Method-All* (using all patches of a sample) for the WI and WV on databases D_c and D_{uc} . This validates the necessity of highly idiosyncratic patches in our task.

2) *Ablating Reinforcement Learning*: Now, we check the requirement of the RL for highly IdS patch detection. In [11], Inception module [50]-based deep features were used for IdS patch detection which did not work well when compared with our RL-based model in TABLE VIII.

Our RL strategy explores a handwritten sample to find the IdS patch location automatically by exploiting the gathered knowledge. To validate the requirement of RL, we ablate the RL-based automated patch-location finding strategy. Alternatively, we use a sliding window-based protocol which finds all the patches. We then employ ResNet-50 (up to the "avg pool" layer) [28] to extract deep features from every patch, and perform a regression analysis to produce the corresponding IdS score. The top k IdS score-based patches are chosen to inspect the writer. We refer to the method that ablates RL as *Method-Ablate_RL*. In TABLE XII, we compare this method with our proposed method on D_c and D_{uc} using similar experimental setups as in Sections VI-C, VI-D when $k = 100$. *Method-Ablate_RL* employed Inception-ResNet-v2 as I-net similar to our proposed method for WI and WV. *Method-Ablate_RL* also used MAF for feature aggregation and a triplet network for similarity learning like our proposed method for WV. From TABLE XII, we note that our proposed RL-based method performs better than *Method-Ablate_RL* for WI/WV. We observe *Method-Ablate_RL* restricts the independent finding of patch location. Furthermore, *Method-Ablate_RL* is around six times computationally slower than our proposed RL-based method due to locating all patches in the initial stage, when tested on D_c and D_{uc} . This signifies the requirement of RL for idiosyncrasy analysis.

TABLE XII: Ablation study: reinforcement learning

| Writer Inspection | DB | Method | 3-tuple accuracy (%) | | |
|-------------------|----------|-----------|----------------------|--------------|--------------|
| | | | AE_{smv} | AE_{sfv} | AE_{mfv} |
| WI | D_c | Ablate_RL | 80.94 | 72.37 | 76.96 |
| | | Proposed | 88.37 | 81.57 | 84.51 |
| | D_{uc} | Ablate_RL | 79.14 | 70.94 | 75.74 |
| | | Proposed | 87.25 | 79.67 | 82.61 |
| WV | D_c | Ablate_RL | 88.01 | 77.52 | 83.12 |
| | | Proposed | 94.87 | 86.78 | 92.12 |
| | D_{uc} | Ablate_RL | 86.33 | 75.96 | 82.47 |
| | | Proposed | 92.45 | 86.35 | 90.97 |

VII. CONCLUSION

In this paper, we worked on WI and WV from intra-variable handwriting. Inspecting the writer's scribbling on a whole page did not produce good performance. Therefore, we first planned to detect some highly idiosyncratic patches, then performed the inspection from these patches. For such patch detection, we used a recurrent reinforcement learning-based technique, where the idiosyncratic score was predicted by deep feature-based regression analysis. WI and WV were performed by

deep neural architectures. We employed two databases D_c and D_{uc} for the experimental study. Our idiosyncrasy analyzer fostered a promising performance for the writer inspection system. For WI, we obtained the best Top-1 3-tuple accuracy of (88.37%, 81.57%, 84.51%) and (87.25%, 79.67%, 82.61%) on the D_c and D_{uc} databases, respectively. For WV, our system attained the best 3-tuple accuracy of (94.87%, 86.78%, 92.12%) and (92.45%, 86.35%, 90.97%) on D_c and D_{uc} , respectively.

In the future, we will endeavor to generate the intra-variable writing synthetically, so that our system can learn various types of possible intra-variability of individual handwriting. Moreover, we will try to explore some implicit characteristics of handwritten strokes which may not change drastically due to intra-variability.

REFERENCES

- [1] R. N. Morris, *Forensic Handwriting Identification: Fundamental Concepts and Principles*. Academic Press Inc., 2000.
- [2] J. E. Costain, "Questioned Documents and the Law: Handwriting Evidence in the Federal Court System," *Journal of Forensic Sciences*, vol. 22, no. 4, pp. 799–806, 1977.
- [3] M. Bulacu, L. Schomaker, "Text-Independent Writer Identification and Verification Using Textural and Allographic Features," *IEEE Trans. on PAMI*, vol. 29, no. 4, pp. 701–717, 2007.
- [4] M. Z. Alom et al., "The History Began from AlexNet: A Comprehensive Survey on Deep Learning Approaches," *arXiv:1803.01164*, 2018.
- [5] Y.-J. Xiong, Y. Lu, P. S. P. Wang, "Off-line Text-Independent Writer Recognition: A Survey," *Int. J. of Pattern Recognition and Artificial Intelligence*, vol. 31, no. 05, #1756008, 2017.
- [6] C. Adak, B. B. Chaudhuri, M. Blumenstein, "An Empirical Study on Writer Identification and Verification from Intra-variable Individual Handwriting," *IEEE Access*, vol. 7, no. 1, pp. 24 738–24 758, 2019.
- [7] K. M. Koppenhaver, *Factors that Cause Changes in Handwriting*. Humana Press, New Jersey, 2007, ch. 3 of Forensic Document Examination: Principles and Practice, pp. 27–36.
- [8] J. Walton, "Handwriting Changes Due to Aging and Parkinson's Syndrome," *Forensic Science International*, vol. 88, no. 3, pp. 197–214, 1997.
- [9] J. Behrendt, "Alzheimer's Disease and Its Effect on Handwriting," *Journal of Forensic Sciences*, vol. 29, no. 1, pp. 87–91, 1984.
- [10] M. Diaz, M. A. Ferrer, D. Impedovo, M. I. Malik, G. Pirlo, R. Plamondon, "A Perspective Analysis of Handwritten Signature Technology," *ACM Computing Surveys*, vol. 51, no. 6, article 117, 2019.
- [11] C. Adak, B. B. Chaudhuri, M. Blumenstein, "A Study on Idiosyncratic Handwriting with Impact on Writer Identification," *ICFHR*, pp. 193–198, 2018.
- [12] S. Lathuiliere, P. Mesejo, X. A.-Pineda, R. Horaud, "A Comprehensive Analysis of Deep Regression," *IEEE Trans. on PAMI*, 2019.
- [13] R. S. Sutton, A. G. Barto, *Reinforcement Learning: An Introduction*. MIT Press, Cambridge, MA, 2018, p. 2nd eds.
- [14] R. Plamondon, G. Lorette, "Automatic Signature Verification and Writer Identification - The State of the Art," *Pattern Recognition*, vol. 22, no. 2, pp. 107–131, 1989.
- [15] S. N. Srihari, S.-H. Cha, H. Arora, S. Lee, "Individuality of Handwriting," *Journal of Forensic Sciences*, vol. 47, no. 4, pp. 856–872, 2002.
- [16] S. He, L. Schomaker, "Writer Identification Using Curvature-Free Features," *Pattern Recognition*, vol. 63, pp. 451–464, 2017.
- [17] X. Wu, Y. Tang, W. Bu, "Offline Text-Independent Writer Identification Based on Scale Invariant Feature Transform," *IEEE Trans. on Information Forensics and Security*, vol. 9, no. 3, pp. 526–536, 2014.
- [18] D. Bertolini, L. S. Oliveira, E. Justino, R. Sabourin, "Texture-based Descriptors for Writer Identification and Verification," *Expert Systems with Applications*, vol. 40, pp. 2069–2080, 2013.
- [19] A. Nicolaou, A. D. Bagdanov, M. Liwicki, D. Karatzas, "Sparse Radial Sampling LBP for Writer Identification," *ICDAR*, pp. 716–720, 2015.
- [20] A. J. Newell, L. D. Griffin, "Writer Identification using oriented Basic Image Features and the Delta Encoding," *Pattern Recognition*, vol. 47, no. 6, pp. 2255–2265, 2014.
- [21] R. Jain, D. Doermann, "Offline Writer Identification Using K-Adjacent Segments," *ICDAR*, pp. 769–773, 2011.

- [22] V. Christlein, D. Bernecker, E. Angelopoulou, "Writer Identification Using VLAD Encoded Contour-Zernike Moments," *ICDAR*, pp. 906–910, 2015.
- [23] V. Christlein, D. Bernecker, A. Maier, E. Angelopoulou, "Offline Writer Identification Using Convolutional Neural Network Activation Features," *German Conference on Pattern Recognition*, pp. 540–552, 2015.
- [24] Y. Tang, X. Wu, "Text-Independent Writer Identification via CNN Features and Joint Bayesian," *ICFHR*, pp. 566–571, 2016.
- [25] S. He, L. Schomaker, "Deep Adaptive Learning for Writer Identification based on Single Handwritten Word Images," *Pattern Recognition*, vol. 88, pp. 64–74, April, 2019.
- [26] S. Fiel, R. Sablatnig, "Writer Identification and Retrieval Using a Convolutional Neural Network," *Int. Conf. on Computer Analysis of Images and Patterns*, pp. 26–37, 2015.
- [27] Q. H.-Thu, M. N. Garcia, F. Speranza, P. Corriveau, A. Raake, "Study of Rating Scales for Subjective Quality Assessment of High-Definition Video," *IEEE Trans. on Broadcasting*, vol. 57, no. 1, pp. 1–14, 2011.
- [28] K. He, X. Zhang, S. Ren, J. Sun, "Deep Residual Learning for Image Recognition," *CVPR*, pp. 770–778, 2016.
- [29] O. Russakovsky et al., "ImageNet Large Scale Visual Recognition Challenge," *Int. J. Comput. Vis.*, vol. 115, no. 3, pp. 211–252, 2015.
- [30] K. Simonyan, A. Zisserman, "Very Deep Convolutional Networks for Large-Scale Image Recognition," *ICLR*, 2015.
- [31] K. Cho et al., "Learning Phrase Representations using RNN Encoder-Decoder for Statistical Machine Translation," *Empirical Methods in Natural Language Processing (EMNLP)*, pp. 1724–1734, 2014.
- [32] V. Mnih, N. Heess, A. Graves, K. Kavukcuoglu, "Recurrent Models of Visual Attention," *NIPS*, pp. 2204–2212, 2014.
- [33] R. J. Williams, "Simple Statistical Gradient-Following Algorithms for Connectionist Reinforcement Learning," *Machine Learning*, vol. 8, no. 3-4, pp. 229–256, 1992.
- [34] D. Wierstra, A. Foerster, J. Peters, J. Schmidhuber, "Solving Deep Memory POMDPs with Recurrent Policy Gradients," *Int. Conf. on Artificial Neural Networks (ICANN)*, pp. 697–706, 2007.
- [35] R. S. Sutton, D. McAllester, S. Singh, Y. Mansour, "Policy Gradient Methods for Reinforcement Learning with Function Approximation," *NIPS*, pp. 1057–1063, 1999.
- [36] F. Chollet, "Xception: Deep Learning with Depthwise Separable Convolutions," *CVPR*, pp. 1800–1807, 2017.
- [37] C. Szegedy, S. Ioffe, V. Vanhoucke, A. Alemi, "Inception-v4, Inception-ResNet and the Impact of Residual Connections on Learning," *AAAI*, pp. 4278–4284, 2017.
- [38] N. Srivastava, G. Hinton, A. Krizhevsky, I. Sutskever, R. Salakhutdinov, "Dropout: A Simple Way to Prevent Neural Networks from Overfitting," *Journal of Machine Learning Research*, pp. 1929–1958, 2014.
- [39] I. Goodfellow, Y. Bengio, A. Courville, *Deep Learning*. MIT Press, 2016, <http://www.deeplearningbook.org>.
- [40] E. Hoffer, N. Ailon, "Deep Metric Learning Using Triplet Network," *Int. Workshop on Similarity-Based Pattern Recognition*, pp. 84–92, 2015.
- [41] F. Schroff, D. Kalenichenko, J. Philbin, "Facenet: A Unified Embedding for Face Recognition and Clustering," *CVPR*, pp. 815–823, 2015.
- [42] A. Hermans, L. Beyer, B. Leibe, "In Defense of the Triplet Loss for Person Re-Identification," *arXiv:1703.07737*, 2017.
- [43] J. Bromley, I. Guyon, Y. LeCun, E. Sackinger, R. Shah, "Signature Verification Using A Siamese Time Delay Neural Network," *NIPS*, pp. 737–744, 1993.
- [44] K. H. Brodersen, C. S. Ong, K. E. Stephan, J. M. Buhmann, "The Balanced Accuracy and Its Posterior Distribution," *ICPR*, pp. 3121–3124, 2010.
- [45] A. Naftali, "Behavior Factors in Handwriting Identification," *The Journal of Criminal Law, Criminology and Police Science*, vol. 56, no. 4, pp. 528–539, 1965.
- [46] M. Diaz, M. A. Ferrer, G. S. Eskander, R. Sabourin, "Generation of Duplicated Off-Line Signature Images for Verification Systems," *IEEE Trans. on PAMI*, vol. 39, no. 5, pp. 951–964, 2017.
- [47] M. Diaz, M. A. Ferrer, R. Sabourin, "Approaching the Intra-Class Variability in Multi-Script Static Signature Evaluation," *ICPR*, pp. 1147–1152, 2016.
- [48] M. Everingham et al., "The Pascal Visual Object Classes Challenge: A Retrospective," *International Journal of Computer Vision*, vol. 111, no. 1, pp. 98–136, 2015.
- [49] R. Meyers, M. Lu, C. W. de Puiseau, T. Meisen, "Ablation Studies in Artificial Neural Networks," *arXiv:1901.08644*, 2019.
- [50] C. Szegedy et al., "Going Deeper with Convolutions," *CVPR*, pp. 1–9, 2015.



Chandranath Adak (S'13, M'20) received his PhD in analytics from University of Technology Sydney, Australia in 2019. Currently, he is an Assistant Professor at Centre for Data Science, IIS Institute of Advanced Studies and Research, India. His research interests include image processing, pattern recognition, document image analysis, and machine learning-related subjects.



Bidyut B. Chaudhuri (F'01, LF'16) received his PhD from Indian Institute of Technology, Kanpur in 1980. He joined the Indian Statistical Institute in 1978, and retired from the regular position in 2015. Currently, he is the Pro-Vice-Chancellor (Academic) of Techno India University, West Bengal, India. His research interests include pattern recognition, machine learning, digital document processing, natural language processing, speech processing, etc.



Chin-Teng Lin (F'05) received his PhD in electrical engineering from Purdue University, USA in 1992. He is currently a Distinguished Professor of CAI, FEIT, University of Technology Sydney, Chair Professor of Electrical and Computer Engg., NCTU, and Honorary Professor of University of Nottingham. His research interests include computational intelligence, fuzzy neural networks, brain-computer interface, robotics, etc.



Michael Blumenstein (SM'13) received his PhD in computational intelligence from Griffith University, Australia in 2001. He is currently a Professor and the Associate Dean (Research Strategy and Management) with the FEIT, University of Technology Sydney, Australia. His research interests include pattern recognition, artificial intelligence, video processing, document image processing, environmental science, neurobiology, coastal management, etc.

APPENDIX A
ALGORITHMS

Refer to Section V and Fig. 5.

Algorithm 1 MAF: *page_level_Mean_Aggregated_Feature*

```

1: Input:  $p'_j : \{p'_1, p'_2, \dots, p'_k\}$  | top- $k$  idiosyncratic patches
   in a page image  $H$ ;
2: Output:  $v^{(\mu)} : \{v_1^\mu, v_2^\mu, \dots, v_q^\mu\}$  | a  $q$ -dimensional feature
   vector representing page image  $H$ ;
3: for  $j = 1$  to  $k$  do
4:    $v^{(j)} = \text{I-net}(p'_j)$ ; ▷ Comment:
    $v^{(j)} := \{v_1^j, v_2^j, \dots, v_q^j\} := \{v_x^j; \forall x = 1, 2, \dots, q\}$ 
5: end for
6:  $v^{(\mu)} = \text{NULL}$ ;
7: for  $x = 1$  to  $q$  do
8:    $Sum = 0$ ;
9:   for  $j = 1$  to  $k$  do
10:     $Sum = Sum + v_x^j$ ;
11:   end for
12:    $v_x^\mu = Sum/k$ ;
13:    $v^{(\mu)} = v^{(\mu)}.append(v_x^\mu)$ ;
14: end for
15: return  $v^{(\mu)}$ ;

```

Algorithm 2 XAF: *page_level_max_Aggregated_Feature*

```

1: Input:  $p'_j : \{p'_1, p'_2, \dots, p'_k\}$  | top- $k$  idiosyncratic patches
   in a page image  $H$ ;
2: Output:  $v^{(\mu)} : \{v_1^\mu, v_2^\mu, \dots, v_q^\mu\}$  | a  $q$ -dimensional feature
   vector representing page image  $H$ ;
3: for  $j = 1$  to  $k$  do
4:    $v^{(j)} = \text{I-net}(p'_j)$ ; ▷ Comment:
    $v^{(j)} := \{v_1^j, v_2^j, \dots, v_q^j\} := \{v_x^j; \forall x = 1, 2, \dots, q\}$ 
5: end for
6:  $v^{(\mu)} = \text{NULL}$ ;
7: for  $x = 1$  to  $q$  do
8:    $Max = v_x^1$ ;
9:   for  $j = 2$  to  $k$  do
10:    if  $v_x^j > Max$  then
11:       $Max = v_x^j$ ;
12:    end if
13:   end for
14:    $v_x^\mu = Max$ ;
15:    $v^{(\mu)} = v^{(\mu)}.append(v_x^\mu)$ ;
16: end for
17: return  $v^{(\mu)}$ ;

```
